

Article

Down-Regulation of Photosynthesis to Elevated CO₂ and N Fertilization in Understory *Fraxinus rhynchophylla* Seedlings

Syeon Byeon ¹, Kunhyo Kim ¹, Jeonghyun Hong ¹, Seohyun Kim ¹, Sukyung Kim ¹, Chanoh Park ¹, Daun Ryu ², Sim-Hee Han ³, Changyoung Oh ³ and Hyun Seok Kim ^{1,2,4,5,*}

¹ Department of Agriculture, Forestry and Bioresources, College of Agriculture and Life Sciences, Seoul National University, Seoul 08826, Korea; sybyun419@gmail.com (S.B.); kunhyokim94@snu.ac.kr (K.K.); august_2@snu.ac.kr (J.H.); shkim0718@snu.ac.kr (S.K.); bluemoon023@naver.com (S.K.); qkrcksg1223@snu.ac.kr (C.P.)

² Interdisciplinary Program in Agricultural and Forest Meteorology, College of Agriculture and Life Sciences, Seoul National University, Seoul 08826, Korea; aldoi0314@gmail.com

³ Department of Forest Bioresources, National Institute of Forest Science, Suwon 16631, Korea; simhee02@korea.kr (S.-H.H.); happyohcy@korea.kr (C.O.)

⁴ National Center for Agro Meteorology, Seoul 08826, Korea

⁵ Research Institute for Agriculture and Life Sciences, College of Agriculture and Life Sciences, Seoul National University, Seoul 08826, Korea

* Correspondence: cameroncrazies@snu.ac.kr; Tel.: +82-10-8876-0423



Citation: Byeon, S.; Kim, K.; Hong, J.; Kim, S.; Kim, S.; Park, C.; Ryu, D.; Han, S.-H.; Oh, C.; Kim, H.S. Down-Regulation of Photosynthesis to Elevated CO₂ and N Fertilization in Understory *Fraxinus rhynchophylla* Seedlings. *Forests* **2021**, *12*, 1197. <https://doi.org/10.3390/f12091197>

Academic Editors: Dilek Killi, Carlos Gonza-lez-Benecke, Elif Aylin Ozudogru, Francesca Ugolini and Jonathan Cumming

Received: 16 July 2021

Accepted: 31 August 2021

Published: 3 September 2021

Publisher's Note: MDPI stays neutral with regard to jurisdictional claims in published maps and institutional affiliations.



Copyright: © 2021 by the authors. Licensee MDPI, Basel, Switzerland. This article is an open access article distributed under the terms and conditions of the Creative Commons Attribution (CC BY) license (<https://creativecommons.org/licenses/by/4.0/>).

Abstract: (1) Background: Down-regulation of photosynthesis has been commonly reported in elevated CO₂ (eCO₂) experiments and is accompanied by a reduction of leaf nitrogen (N) concentration. Decreased N concentrations in plant tissues under eCO₂ can be attributed to an increase in nonstructural carbohydrate (NSC) and are possibly related to N availability. (2) Methods: To examine whether the reduction of leaf N concentration under eCO₂ is related to N availability, we investigated understory *Fraxinus rhynchophylla* seedlings grown under three different CO₂ conditions (ambient, 400 ppm [aCO₂]; ambient × 1.4, 560 ppm [eCO₂1.4]; and ambient × 1.8, 720 ppm [eCO₂1.8]) and three different N concentrations for 2 years. (3) Results: Leaf and stem biomass did not change under eCO₂ conditions, whereas leaf production and stem and branch biomass were increased by N fertilization. Unlike biomass, the light-saturated photosynthetic rate and photosynthetic N-use efficiency (PNUE) increased under eCO₂ conditions. However, leaf N, Rubisco, and chlorophyll decreased under eCO₂ conditions in both N-fertilized and unfertilized treatments. Contrary to the previous studies, leaf NSC decreased under eCO₂ conditions. Unlike leaf N concentration, N concentration of the stem under eCO₂ conditions was higher than that under ambient CO₂ (4). Conclusions: Leaf N concentration was not reduced by NSC under eCO₂ conditions in the understory, and unlike other organs, leaf N concentration might be reduced due to increased PNUE.

Keywords: photosynthesis; understory; leaf nitrogen content; Rubisco; nonsturctural carbohydrates; nitrogen addition

1. Introduction

The primary effect of rising atmospheric carbon dioxide (CO₂) concentration on plants is an increase in the photosynthetic rate. C₃ plants show significantly stimulated carbon assimilation and enhanced growth under elevated CO₂ (eCO₂) conditions [1–3]; however, many studies claim that plants cannot sustain the stimulation of biomass accumulation, which would result under long-term CO₂ fumigation [2,4]. The uncertainties in the sustainability of enhanced productivity and carbon (C) storage under elevated CO₂ (eCO₂) conditions are because of different nutrient conditions [5,6]. For example, productivity enhancement decreased with time as nitrogen (N) availability decreased at the Oak Ridge FACE site [4]. A suboptimal N supply can lead to the down-regulation of photosynthesis [7].

Down-regulation of photosynthesis is commonly reported in eCO₂ experiments. This phenomenon involves a reduction in the maximum carboxylation rate (V_{Cmax}) and maximum electron transport rate driving ribulose biphosphate (RuBP) regeneration (J_{max}). It is associated with reduced leaf N concentration [3,8] because a large fraction of leaf N concentration is invested in the photosynthetic apparatus [9]. Many researchers have suggested that accumulated nonstructural carbohydrates (NSC) dilute leaf N concentration to balance sink–source organs [10]. Reduced leaf N concentration can be attributed to dilution by additional photosynthates, such as NSC, resulting from a “sink–source imbalance,” i.e., an incapacity to form a sufficient “sink” [10,11]. “Sink organs” are plant parts that use photosynthates in storage, construction, and respiration. Plants with large sink organs exhibit little down-regulation despite growing under eCO₂ conditions because the NSC can be translocated to the sink organs. In a study on poplar, free-air CO₂ enrichment (POP-FACE), down-regulation of V_{Cmax} occurred only in *Populus alba*, which had the smallest sink (diameter growth) among the three poplar clones [12].

Down-regulation of photosynthesis occurs because accumulated NSC suppress the gene expression of Rubisco [10,13], and whereas NSC accumulation is accelerated under eCO₂ conditions and low N availability [14]. Previous studies have suggested that photosynthesis down-regulation is mitigated under eCO₂ conditions at high N concentration [3,15]. Rubisco suppression under eCO₂ conditions is associated with leaf N reallocation from a non-limiting source to other limiting photosynthetic components, such as the light-harvesting complex [9,16]. This change in N allocation can provide an opportunity to increase photosynthetic N use efficiency (PNUE), which is defined as the net C assimilation rate per unit leaf N [8] and is associated with the enhanced efficiency of Rubisco due to photorespiration suppression under eCO₂ conditions [17,18]. However, to the best of our knowledge, there has been no investigation of changes in leaf N allocation in woody plants under different N availability conditions under eCO₂ conditions.

In contrast, N reduction also occurs in other sink organs apart from leaves [19–21]. For example, the N concentration in the edible parts of major food crops decreased by 9%–15% [20], whereas that aboveground in wheat decreased by 23% [21]. N reduction in sink organs can be regarded as a dilution of NSC accumulation [19]. In a previous meta-analysis, the average concentration of soluble sugars and starch in aboveground woody parts significantly increased by 38.6% and 9.9%, respectively. In roots, starch (9.8%) concentration significantly increased under elevated CO₂ conditions, whereas soluble sugar concentration decreased by 6.7% but not significantly [22]. The effect of eCO₂ on leaf N dilution can be reduced by N fertilization [20,23]; thus, it can be speculated whether NSC changes can be attributed to N concentration variations in other sink organs under different CO₂ and N conditions.

Most previous studies have focused on the effects of elevated CO₂ on dominant overstory trees (Souza et al., 2010), whereas few studies have investigated the effects of interactions of CO₂ and nutrients on understory tree physiological characteristics [24–27], although the understory contribution to the forest carbon balance is substantial [28,29]. To investigate how the combination of N fertilization and eCO₂ administered to seedlings in the understory affects the N concentrations of sink and source organs and the down-regulation of photosynthesis, we exposed understory *Fraxinus rhynchophylla* seedlings to three different CO₂ concentrations (ambient, ~400 ppm [aCO₂]; ambient × 1.4 ppm, 560 ppm [eCO₂1.4]; and ambient × 1.8, 720 ppm [eCO₂1.8]) and three different N treatments (unfertilized: 2.98 gN m⁻² yr⁻¹, N1 + 5.6 gN m⁻² yr⁻¹, and N1 + 11.2 gN m⁻² yr⁻¹) using an open-top chamber (OTC) for 2 years. *F. rhynchophylla* is a deciduous tree mainly distributed in East Asia and an economically important species. This research proposes three hypotheses to further understanding between photosynthesis, NSC and N condition:

- Down-regulation of photosynthesis under eCO₂ occurs in low N availability.
- Leaf N allocation changes with different N and CO₂ concentrations.
- Dilution occur other organs changes with different N availability under eCO₂.

2. Materials and Methods

2.1. Study Site

The study was conducted using an OTC at the National Institute of Forest Science ($37^{\circ}15'04''$ N, $136^{\circ}57'59''$ E) in South Korea. The mean annual temperature is 13.0°C , and the annual precipitation is 1271.2 mm (19 May 2020, <https://data.kma.go.kr/>). The OTC experiment utilized three decagonal chambers (10 m in diameter and 7 m in height) with different atmospheric CO₂ concentrations: ambient, 400 ppm (aCO₂); ambient \times 1.4, 560 ppm (eCO₂1.4); and ambient \times 1.8, 720 ppm (one OTC per treatment). Two eCO₂ concentrations have been predicted for 2050 and 2070 by the IPCC [30]. A 0.15-mm-thick polyolefin film with a light transmittance of approximately 88% and chemical and water resistance formed the outer covering material. The CO₂ exposure device consisted of 16 cylindrical discharge polyvinyl chloride pipes in each chamber (height: 1.5 m, diameter: 10 cm), vertically connected to the pipe, thus exposing the plants to CO₂. The CO₂ concentrations in the chambers were measured using an infrared gas analyzer (ZRH type, Fuji Electric System Co. Ltd., Tokyo, Japan), and the CO₂ concentrations inside were controlled by mixing pure liquefied CO₂ from 8:00 a.m. to 6:00 p.m. [31]. The overstory canopy comprised six temperate species. Three seedlings of 4-year-old *Pinus densiflora* Siebold & Zucc and 2-year-old *Fraxinus rhynchophylla* HANCE, *Quercus acutissima*, *Acer pseudosieboldianum* (Pax) Kom., *Crataegus pinnatifida* for. *pinnatifida*, and *Sorbus alnifolia* Siebold & Zucc Koch were planted in September 2009. The density within the OTC was 2547 trees ha⁻¹. The leaf area index was 0.28 ± 0.06 , 0.34 ± 0.07 , and $0.46 \pm 0.07\text{ m}^2\text{ m}^{-2}$ under aCO₂, eCO₂1.4, and eCO₂1.8, respectively, using leaf litter collection methods [32] in 2017 ($p = 0.166$).

Seedlings of 2-year-old *F. rhynchophylla* were transplanted into 10 L pots filled with a 1:1:1 mixture of cocopeat: peat moss: vermiculite and exposed to three different CO₂ treatments using the OTCs in March 2019. Plants were fertilized monthly from May to July for 2 years with NH₄NO₃, as follows: unfertilized treatment (N1), 5.6 gN m⁻² yr⁻¹ (N2), or 11.2 gN m⁻² yr⁻¹ (N3) [33]. There were five replicate seedlings in each N fertilization system and a total of 15 replicate seedlings in each CO₂ treatment (5 replications \times 3 N concentrations). Furthermore, *F. rhynchophylla* is a deciduous temperate species; the average height of the seedlings was 59.64 ± 0.76 cm, and the diameter was 9.23 ± 0.29 cm in 2019.

2.2. Leaf Gas Exchange Measurements and Sample Collection

A portable gas exchange system (LI-6400, LI-COR, Lincoln, NE, USA) was used to measure the light-saturated photosynthetic rate (A_{\max}) between 08:00 and 14:00, at a leaf temperature of 25°C in July in 2019 and July and September in 2020. A light response curve was generated by changing the photosynthetic photon flux density in the following order: 1400, 1200, 1000, 800, 600, 400, 200, 100, 75, 50, 25, 0, and 1200 $\mu\text{mol m}^{-2}\text{ s}^{-1}$. The CO₂ samples were set at 400, 560, and 720 $\mu\text{mol mol}^{-1}$ for growth under CO₂ conditions (aCO₂, eCO₂1.4, and eCO₂1.8), respectively. The light-saturated photosynthetic rate (A_{\max}) was estimated by selecting the highest photosynthesis value under light-saturated irradiance from the light response curve. The maximum carboxylation rate (V_{Cmax}) and RuBP regeneration rates (J_{\max}) were measured in July 2019 and 2020 by plotting A/C_i curves under irradiance (1200 $\mu\text{mol m}^{-2}\text{ s}^{-1}$), which is the optimal irradiance for Rubisco activity [34,35]. The change in the reference CO₂ concentrations for each chamber were in the following order: aCO₂: 400, 300, 200, 100, 75, 50, 25, 0, 400, 400, 600, 800, 1000, and 1200 $\mu\text{mol m}^{-2}\text{ s}^{-1}$; eCO₂ 1.4: 560, 400, 300, 200, 100, 75, 50, 25, 0, 560, 560, 800, 1000, and 1200 $\mu\text{mol m}^{-2}\text{ s}^{-1}$; and eCO₂ 1.8: 720, 600, 400, 300, 200, 100, 75, 50, 25, 0, 720, 720, 100, and 1200 $\mu\text{mol m}^{-2}\text{ s}^{-1}$. The V_{Cmax} and J_{\max} were estimated using the curve fitting model of version 2.0 developed by Sharkey [36].

Three leaves were collected (three leaves \times five replicates \times three N treatments in each treatment), including one for leaf gas exchange and two leaves nearby in July 2019 and July and September 2020. To measure NSC, the N per unit area (N_{area} , g m⁻²), N per unit mass (N_{mass} , g m⁻²), Rubisco (g m⁻²), and chlorophyll (g m⁻²), leaf discs with 1-cm diameter

were punched out, excluding the midrib, and stored in a liquid nitrogen tank (-196°C). The dried samples at 70°C were powdered using a homogenizer (FastPrep-24, MP Biomedicals, Solon, OH), and leaf N concentration was measured using a CHNS-Analyzer Flash EA 1112 (Thermo Electron Corporation, Massachusetts, USA) at NICEM, Seoul National University. PNUE ($\mu\text{mol N}^{-1} \text{s}^{-1}$) was calculated as the ratio of A_{\max} to N_{area} .

The seedlings were harvested and sectioned into leaves, stems, branches, and roots in September 2020 to evaluate biomass allocation to determine their dry weights, and the root, stem, and stem and root N_{mass} were estimated using the same methods as those for leaf N concentrations.

2.3. Total Nonstructural Carbohydrates

Three discs of leaves and 15–20 mg of root and stem were ground, and the ground samples were used to measure the NSC (sum of the soluble sugars and starch). The soluble sugars were extracted with 1.5 mL of 80% (*v/v*) ethanol in a water bath at 80°C for 30 min. After 10 min of centrifugation at $14,000 \times g$, the soluble sugar concentration was determined colorimetrically at 490 nm using the phenol-sulfuric method [37]. Starch was extracted from the remaining pellets after measuring the sugar concentrations. The pellet was incubated in 2.5 mL sodium acetate buffer (0.2 M) in a 100°C water bath for 1 h. After cooling to room temperature, 2 mL of the buffer and 1 mL of amyloglucosidase (0.5% by weight, Sigma A9229-1G) were added. The mixed samples were incubated overnight in a water bath at 55°C . After 10 min of centrifugation at $14,000 \times g$, the starch concentration was determined colorimetrically at 490 nm using the phenol-sulfuric method.

2.4. Measurement of Rubisco and Chlorophyll Contents

Rubisco was extracted from leaf discs stored at -80°C , and Rubisco content on an area basis was determined using sodium dodecyl sulphate (SDS)-polyacrylamide gel electrophoresis (PAGE) [38]. One leaf disc (0.785 cm^2) was ground using a homogenizer (FastPrep-24, MP Biomedicals, Solon, OH), and samples were extracted in 1 mL of extraction buffer at 4°C . The protein extraction buffer comprised 80 mM Tris-HCl (pH 7.4), 1% (*w/v*) polyvinylpolypyrrolidone, 1.5% (*v/v*) glycerol, 100 mM β -mercaptoethanol, and 20 kg m^{-3} SDS. The samples were centrifuged at $15,000 \times g$ for 30 min at 4°C , denatured at 90°C for 5 min, and subsequently analyzed by SDS-PAGE.

Chlorophyll was extracted using the dimethyl sulfoxide (DMSO) method [39]. The two discs were incubated in a brown bottle containing 5 mL of DMSO at 65°C for 6 h in a water bath. The samples were estimated at two wavelengths, 649 and 665 nm, using a spectrophotometer (Optizen 2120 UV, Mecasys, Korea). The chlorophyll N content was derived using the DMSO equation [40] as follows:

$$\text{Total chlorophyll content } (\mu\text{g mL}^{-1}) = 21.44 A_{649} + 5.97 A_{665} \quad (1)$$

2.5. Statistical Analysis

A three-way repeated-measures ANOVA was performed using the R program (ver. 3.3.2; R Core Team, 2016) for A_{\max} , V_{Cmax} , J_{\max} , leaf N_{mass} , leaf N_{area} , Rubisco, PNUE, NSC, chlorophyll, and chlorophyll:Rubisco. Three-way repeated measures of ANOVA were performed with the fixed factors “CO₂ treatment” and “nitrogen” and the random factor “period.” Two-way ANOVA was conducted on N_{mass} , NSC and biomass of stem and root, and total leaf production to compare the CO₂ and N effects within a period. In repeated-measures ANOVA and two-way ANOVA, when the main factors of CO₂ and N and interaction with CO₂ treatment and N treatment were significant, Tukey’s HSD test was performed to compare the CO₂ and N effects.

3. Results

3.1. Whole Plant Biomass Allocation

There was a significant increase in the aboveground biomass with increased N fertilization, but no effect of CO₂ treatment was observed (Figure 1). Leaf production under N3 condition (8.34 ± 0.83 g) was 43.3% and 61.7% higher than that under N1 (5.82 ± 0.62 g, $p = 0.060$) and N2 (5.16 ± 0.72 g, $p = 0.018$) conditions, respectively (Figure 1a). Stem production also increased with N fertilization, with that under N3 condition being 50.2% higher than that under N1 condition (24.00 ± 3.12 g, $p = 0.011$, Figure 1b). Unlike the aboveground biomass, roots showed no differences with the N treatments (Figure 1c).

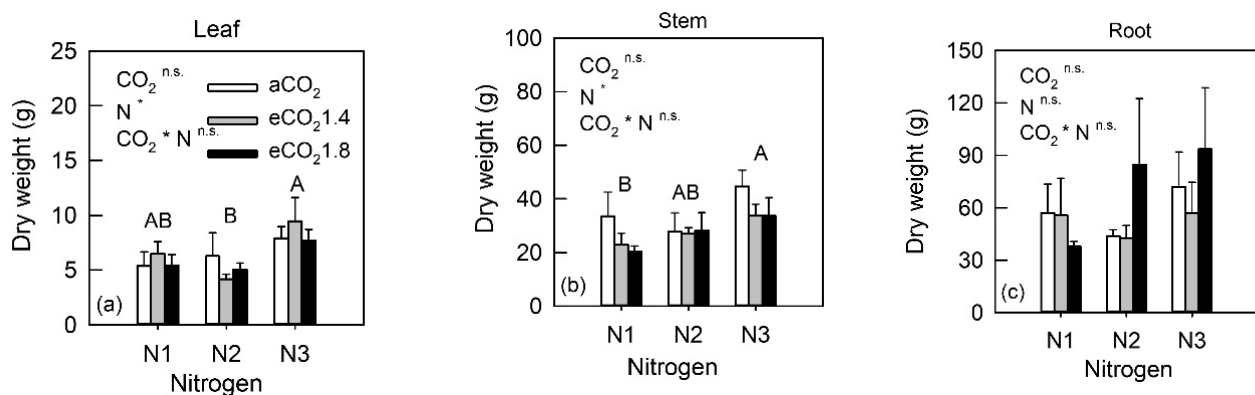


Figure 1. Average dry weight of the (a) leaf, (b) stem and (c) root measured in *Fraxinus rhynchophylla* grown at three different CO₂ chambers (ambient: aCO₂; ambient × 1.4: eCO₂1.4; ambient × 1.8: eCO₂1.8) and three different N treatments (N1: unfertilized, N2: N1 + 5.6 gN m⁻² yr⁻¹ and N3: N1 + 11.2 gN m⁻² yr⁻¹). Results are presented as mean + SE and summary of a two-way ANOVA. In summary of a two-way ANOVA, CO₂ represents CO₂ treatment and N represents nitrogen treatment. The X axis represents N fertilization and CO₂ treatments: aCO₂ (white bar), eCO₂1.4 (grey bar) and eCO₂1.8 (black bar). The significance of the primary effects and their interactions are shown with the abbreviations. n.s., non-significant; *, $p < 0.05$ (two-way ANOVA, CO₂ × N). There were differences between N treatments in dry weight of leaf and stem. Different capital letters indicate significant differences among N treatment and lowercase letters indicate significant differences among CO₂ treatments (Tukey's test, $p < 0.05$).

3.2. Photosynthetic Characteristics and Nonstructural Carbohydrates

Elevated CO₂ exposure increased the light-saturated photosynthetic rate (A_{\max}), and there was no N fertilization effect or interaction effect between N and CO₂ treatments (Table 1). The average A_{\max} was 20.1% and 31.0% higher under eCO₂1.4 ($p = 0.036$) and eCO₂1.8 ($p < 0.001$) conditions than under aCO₂ condition, respectively, whereas A_{\max} showed an increasing tendency under eCO₂ conditions compared with that under aCO₂ condition in all N treatments, although the difference was not significant (Table 2). Unlike A_{\max} , down-regulation of other photosynthetic characteristics occurred, including J_{\max} , leaf N concentration, Rubisco content, and chlorophyll content (Table 1). The average J_{\max} under eCO₂1.8 was 20.9% and 18.0% lower than that under eCO₂1.4 condition ($p = 0.002$) and under aCO₂ condition ($p = 0.008$), respectively, and J_{\max} under eCO₂1.8 condition decreased by 32.4% compared with that under aCO₂ condition in N3 (Table 2, $p = 0.012$). Similarly, the average $V_{C\max}$ under eCO₂1.8 showed the lowest value and was lower than that under aCO₂ in all N treatments, but there were only marginal differences in $V_{C\max}$ among CO₂ treatments ($p = 0.083$, Table 2). Leaf N_{mass} decreased under eCO₂ conditions and increased with N fertilization, but there was no interaction between N and CO₂ treatments (Table 1). The average leaf N_{mass} decreased by 9.4% and 15.3% under eCO₂1.4 ($p = 0.035$) and eCO₂1.8 ($p < 0.001$) conditions compared with that under aCO₂ condition, respectively (Table 2). In addition, N_{mass} showed an interaction effect between CO₂ and time period (Table 1); thus, the differences in leaf N_{mass} decreased in September 2020 (Figure 2a). The reduction in leaf N_{mass} under eCO₂1.4 decreased from 21.0% (aCO₂: 2.14 ± 0.08% vs. eCO₂1.4: 1.69 ± 0.09%) in 2019 to no significant decrease in July and

September 2020; similarly, the reduction in leaf N_{mass} under eCO₂1.8 compared with that under aCO₂ was significant in July, 2020 (aCO₂: $1.71 \pm 0.06\%$ vs. eCO₂1.8: $1.27 \pm 0.08\%$, -25.5%) but became non-significant in September 2020. For N treatment, N_{mass} showed incremental changes under both N2 and N3 treatments (N2: $1.69 \pm 0.06\%$, +17.6%, N3: $1.68 \pm 0.06\%$, +17.1%) compared with those under N1 ($1.44 \pm 0.07\%$, maximum $P = 0.002$). Similar to N_{mass} , N_{area} also decreased under eCO₂ conditions (Table 1). The average N_{area} was 15.1% and 24.0% lower under eCO₂1.4 ($p = 0.001$) and eCO₂1.8 ($p < 0.001$) conditions than under aCO₂ condition, respectively (Table 2). Unlike N_{mass} , N_{area} did not show an N-fertilization effect. In addition, there was no interaction between N and CO₂ interaction (Table 1), but N_{area} decreased by 34.3% and 24.8% under eCO₂1.8 condition compared with that under aCO₂ condition in N1 and N2, respectively (Table 2).

Table 1. *p*-Values of a three-way ANOVA across period for maximum photosynthetic rate (A_{max}), maximum carboxylation rate (V_{Cmax}), RuBP regeneration rate (J_{max}), nitrogen per unit mass (N_{mass}), nitrogen per unit area (N_{area}), Rubisco per unit area (Rubisco), nonstructural carbohydrates per unit area (NSC), photosynthetic N use efficiency (PNUE), chlorophyll per unit area (Chlorophyll), and ratio of chlorophyll and Rubisco measured in *Fraxinus rhynchophylla* grown at three different CO₂ chambers (ambient: aCO₂; ambient \times 1.4: eCO₂1.4; ambient \times 1.8: eCO₂1.8) and three different N treatments (N1: unfertilized, N2: N1 + 5.6 gN m⁻² yr⁻¹ and N3: N1 + 11.2 gN m⁻² yr⁻¹).

Effect	df	A_{max}	V_{Cmax}	J_{max}	N_{mass}	N_{area}	Rubisco	NSC	PNUE	Chlorophyll	Chlorophyll: Rubisco
CO ₂	2	0.020	0.083	0.007	<0.001	<0.001	<0.001	<0.001	0.021	<0.001	0.708
N	2	0.297	0.927	0.384	0.021	0.870	0.783	0.256	0.442	0.485	0.813
Period	2	0.167	0.001	0.002	<0.001	<0.001	0.002	<0.001	0.219	<0.001	0.588
CO ₂ \times N	4	0.348	0.249	0.199	0.496	0.913	0.321	0.140	0.631	0.925	0.157
CO ₂ \times Period	4	0.996	0.257	0.219	<0.001	0.117	0.029	0.010	0.063	0.611	0.549
N \times Period	4	0.360	0.117	0.010	0.872	0.542	0.710	0.693	0.192	0.031	0.944

In the table, *p*-values for the repeated-measures ANOVA are in bold when significant ($p < 0.05$).

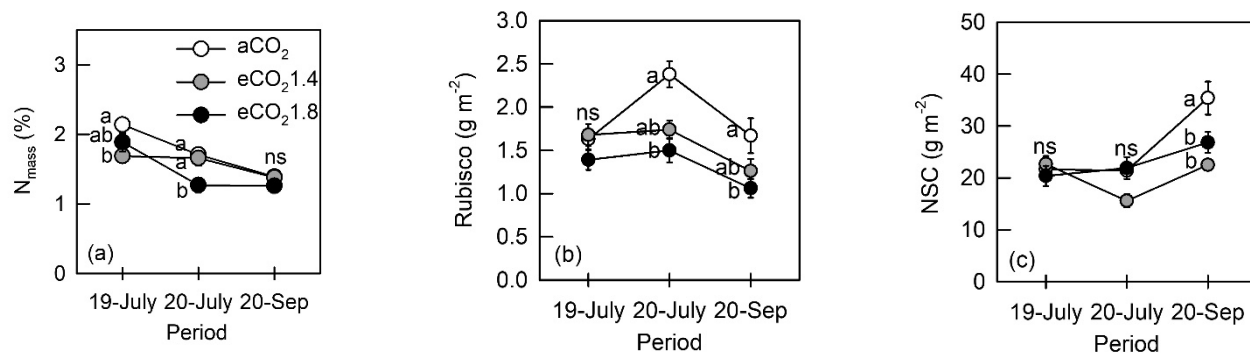


Figure 2. The average of (a) nitrogen per unit mass (N_{mass}) (b) Rubisco per unit area (Rubisco) and (c) nonstructural carbohydrates per unit area (NSC) measured in *Fraxinus rhynchophylla* grown in three different CO₂ chambers (ambient: aCO₂; ambient \times 1.4: eCO₂1.4; ambient \times 1.8: eCO₂1.8) for three periods. Results are presented as mean + SE in each CO₂ treatment: aCO₂ (white circle), eCO₂1.4 (grey circle) and eCO₂1.8 (black circle). The X axis represents period (19-July: July 2019, 20-July: July 2020 and 20-Sep: September 2020). There were interactions between CO₂ \times Period. Different letters indicate significant differences among CO₂ treatments in each period and ns indicate non-significant (Tukey's test, $p < 0.05$).

Table 2. Average \pm standard error of maximum photosynthetic rate (A_{\max}), maximum carboxylation rate ($V_{C\max}$), RuBP regeneration rate (J_{\max}), nitrogen per unit mass (N_{mass}), nitrogen per unit area (N_{area}), Rubisco per unit area (Rubisco), nonstructural carbohydrates per unit area (NSC), photosynthetic N use efficiency (PNUE), chlorophyll per unit area (Chlorophyll) measured in *Fraxinus rhynchophylla* grown at three different CO₂ chambers (ambient: aCO₂; ambient \times 1.4: eCO₂1.4; ambient \times 1.8: eCO₂1.8) and three different N treatments (N1: unfertilized, N2: N1 + 5.6 gN m⁻² yr⁻¹ and N3: N1 + 11.2 gN m⁻² yr⁻¹).

Nitrogen	Chamber	A_{\max} ($\mu\text{mol m}^{-2}\text{s}^{-1}$)	$V_{C\max}$ ($\mu\text{mol m}^{-2}\text{s}^{-1}$)	J_{\max} ($\mu\text{mol m}^{-2}\text{s}^{-1}$)	N_{mass} (%)	N_{area} (g m ⁻²)	Rubisco (g m ⁻²)	NSC (g m ⁻²)	PNUE ($\mu\text{mol molN}^{-1}\text{s}^{-1}$)	Chlorophyll (g m ⁻²)
N1	aCO ₂	5.57 \pm 0.53 ns	35.03 \pm 5.55 ns	58.20 \pm 5.08 ns	1.61 \pm 0.11 ns	0.99 \pm 0.10 a	1.56 \pm 0.12 ns	23.68 \pm 1.58 ns	78.8 \pm 4.4 b	0.15 \pm 0.01 ns
	eCO ₂ 1.4	6.76 \pm 0.70	42.41 \pm 8.68	63.81 \pm 8.89	1.38 \pm 0.11	0.73 \pm 0.07 ab	1.41 \pm 0.13	18.59 \pm 1.28	133.9 \pm 12.1 a	0.13 \pm 0.02
	eCO ₂ 1.8	7.43 \pm 0.91	29.03 \pm 6.52	51.10 \pm 6.66	1.20 \pm 0.17	0.65 \pm 0.08 b	1.18 \pm 0.12	24.69 \pm 2.56	142.0 \pm 17.8 a	0.12 \pm 0.02
N2	aCO ₂	6.77 \pm 0.52 ns	38.45 \pm 7.00 ns	65.66 \pm 4.82 ns	1.85 \pm 0.14 ns	1.01 \pm 0.09 a	1.72 \pm 0.15 ns	24.77 \pm 2.40 ns	95.52 \pm 9.2 b	0.17 \pm 0.01 ns
	eCO ₂ 1.4	8.52 \pm 0.80	37.24 \pm 4.67	70.31 \pm 6.29	1.76 \pm 0.07	1.00 \pm 0.09 ab	1.63 \pm 0.11	20.35 \pm 1.33	130.6 \pm 13.6 ab	0.18 \pm 0.01
	eCO ₂ 1.8	9.19 \pm 0.85	35.78 \pm 4.19	59.21 \pm 5.50	1.55 \pm 0.08	0.80 \pm 0.05 b	1.37 \pm 0.14	21.34 \pm 1.48	158.8 \pm 14.0 a	0.15 \pm 0.01
N3	aCO ₂	7.97 \pm 1.00 ns	42.90 \pm 5.87 ns	75.07 \pm 6.45 a	1.75 \pm 0.15 ns	1.17 \pm 0.08 ns	2.27 \pm 0.20 a	30.67 \pm 3.89 a	97.0 \pm 11.2 b	0.18 \pm 0.01 ns
	eCO ₂ 1.4	9.62 \pm 0.75	50.84 \pm 5.08	72.14 \pm 5.52 ab	1.65 \pm 0.08	0.96 \pm 0.13	1.65 \pm 0.14 ab	22.63 \pm 1.89 b	155.3 \pm 22.1 ab	0.16 \pm 0.02
	eCO ₂ 1.8	10.10 \pm 1.04	23.72 \pm 4.45	50.73 \pm 10.39 b	1.74 \pm 0.15	0.89 \pm 0.04	1.38 \pm 0.11 b	22.97 \pm 2.18 b	154.5 \pm 16.2 a	0.18 \pm 0.01
Average	aCO ₂	6.80 \pm 0.44 b	38.46 \pm 3.47 ns	65.61 \pm 3.30 a	1.74 \pm 0.08 a	1.05 \pm 0.05 a	1.87 \pm 0.11 a	26.26 \pm 1.61 a	90.9 \pm 3.4 b	0.17 \pm 0.01 a
	eCO ₂ 1.4	8.17 \pm 0.47 a	42.69 \pm 4.20	67.96 \pm 4.43 a	1.58 \pm 0.06 b	0.89 \pm 0.06 b	1.57 \pm 0.08 b	20.48 \pm 0.89 b	138.2 \pm 8.7 a	0.16 \pm 0.01 ab
	eCO ₂ 1.8	8.91 \pm 0.55 a	29.73 \pm 3.05	53.79 \pm 4.26 b	1.49 \pm 0.08 b	0.78 \pm 0.04 b	1.31 \pm 0.08 c	23.04 \pm 1.23 ab	151.4 \pm 9.2 a	0.15 \pm 0.01 b

In the table, average of factors \pm their standard errors are shown. Different letters next to the mean indicate significant differences among the CO₂ treatments (Tukey's test, $p < 0.05$). n.s.: non-significant.

Rubisco content decreased under eCO₂ conditions, but there was no N fertilization effect (Table 1). The average Rubisco content decreased with increasing CO₂ concentration (maximum $p = 0.040$) and Rubisco content under eCO₂1.8 condition decreased by 39.0% compared with that under aCO₂ condition in N3 (Table 2, $p < 0.001$). In addition, Rubisco contents showed an interaction between CO₂ and time period (Table 1). Rubisco did not differ with CO₂ concentrations in 2019 but decreases under eCO₂ condition in 2020 (Figure 2b). Rubisco content was 37.0% and 36.5% lower under eCO₂1.8 than under aCO₂ in July (aCO₂: $2.38 \pm 0.15 \text{ g m}^{-2}$, $p = 0.014$) and September (aCO₂: $1.66 \pm 0.20 \text{ g m}^{-2}$, $p < 0.001$), respectively.

To examine the dilution hypothesis and determine whether N fertilization could mitigate the down-regulation of photosynthesis, NSC were quantified in different CO₂ and N treatments. NSC differed depending on the CO₂ treatments and time periods (Table 1). In contrast to previous results of NSC under eCO₂ conditions, the average NSC was 44.5% lower under eCO₂1.4 ($p < 0.001$) than under aCO₂, and the average NSC under eCO₂1.8 tended to be lower than that under aCO₂ but not significantly ($p = 0.061$). Moreover, the reduction in NSC under eCO₂ conditions was noticeably greater in N3 than in the other N treatments (Table 2). The NSC in September ($28.21 \pm 1.51 \text{ g m}^{-2}$) were higher than those in July (2019: $21.58 \pm 0.94 \text{ g m}^{-2}$, 2020: $19.78 \pm 1.02 \text{ g m}^{-2}$, maximum $p < 0.001$). In addition, NSC showed a correlation between CO₂ concentrations and time period (Table 1). There was no reduction in NSC under eCO₂ in July 2019 and 2020, but NSC were reduced by 36.5% and 24.1% under eCO₂1.4 ($p < 0.001$) and eCO₂1.8 ($p < 0.001$) relative to those under aCO₂ ($35.40 \pm 3.19 \text{ g m}^{-2}$) in September 2020 (Figure 2c).

Table 1 shows that PNUE also increased with eCO₂ concentration. The average PNUE was higher under eCO₂1.4 (52.0%, $p < 0.001$) and eCO₂1.8 (66.6%, $p < 0.001$) than under aCO₂, whereas PNUE increased under eCO₂1.8 in all N treatments (Table 2). There was a decrease in the chlorophyll content under eCO₂1.8 compared with that under aCO₂ (Table 1). The chlorophyll content was 11.8% lower under eCO₂1.8 than that under aCO₂ ($p = 0.006$, Table 2). Moreover, the chlorophyll: Rubisco ratio showed no differences between CO₂ treatments (Table 1); thus, there was no leaf N reallocation under eCO₂ conditions and N fertilization treatments.

3.3. Whole-Plant Biochemical Characteristics

Stem N_{mss} was increased under eCO₂ conditions, but there were no differences between the N treatments (Figure 3a). Stem N_{mss} under eCO₂ 1.8 ($0.56 \pm 0.05\%$) increased by 44.9% and 39.7% compared with that under aCO₂ ($p = 0.004$) and eCO₂ 1.4 ($0.40 \pm 0.03\%$, $p = 0.008$), respectively. Although there was no interaction effect between N and CO₂, stem N_{mass} under eCO₂1.8 was 74.1% and 83.5% higher than that under aCO₂ ($p = 0.036$) and eCO₂ 1.4 ($p = 0.020$) in the N3 treatment, respectively. There were no differences in root N_{mass} between CO₂ and N treatments (Figure 3b). For NSC, there was no effect of CO₂ and N treatments, with an interaction effect of only N × CO₂ on the stem. The NSC under eCO₂ 1.4 ($230.08 \pm 56.50 \text{ g}$) decreased by 76.1% compared with that under aCO₂ ($307.99 \pm 28.79 \text{ g}$) only in N2 ($p = 0.006$) (Figure 3c). There were no differences in the root NSC between the CO₂ and nitrogen treatments (Figure 3d).

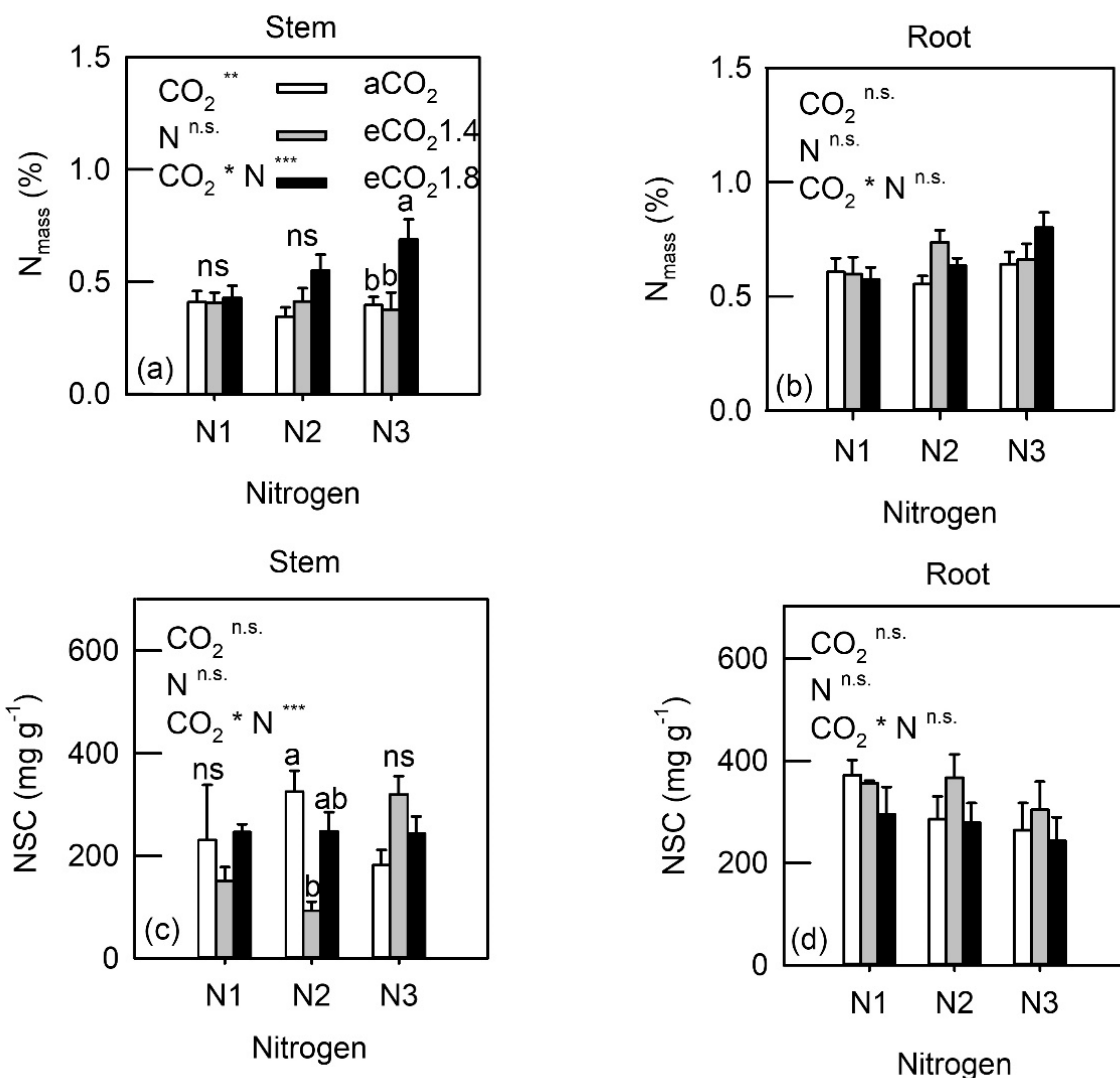


Figure 3. Average of the nitrogen per unit mass (N_{mass}) from (a) stem and (b) root and nonstructural carbohydrates per unit mass (NSC) from (c) stem and (d) root measured in *Fraxinus rhynchophylla* grown at three different CO₂ chambers (ambient: aCO₂; ambient × 1.4: eCO₂ 1.4; ambient × 1.8: eCO₂ 1.8) and three different N treatments (N1: unfertilized, N2: N1 + 5.6 gN m⁻² yr⁻¹ and N3: N1 + 11.2 gN m⁻² yr⁻¹). Results are presented as mean + SE and summary of a two-way ANOVA. In the summary of the two-way ANOVA, CO₂ represents the CO₂ treatment and N represents the nitrogen treatment. The X axis represents N fertilization and CO₂ treatments: aCO₂ (white bar), eCO₂ 1.4 (grey bar) and eCO₂ 1.8 (black bar). The significance of the primary effects and their interactions are shown with the abbreviations. n.s., non-significant; *, p < 0.05; **, p < 0.01; ***, p < 0.001 (two-way ANOVA, CO₂ × N). Different lowercase letters indicate significant differences among CO₂ treatment in each N treatments and capital letters indicate significant differences among N treatment (Tukey's test, p < 0.05).

4. Discussion

4.1. Biomass under eCO₂ and N Fertilization

Biomass enhancement under eCO₂ conditions has been reported in many previous studies [41]. However, the N availability and water status determined the increment of net primary production at the eCO₂ Duke FACE site [42] and Flakaliden [43]. In the understory, the FACE experiment across years reported that the aboveground biomass of the understory community was 25% greater under eCO₂ than under aCO₂ [44]. However, similar to our study, which showed no increase in understory seedling biomass under eCO₂ conditions in any plant part (leaf, stem, or root) (Figure 1), 15 tropical species showed no increase in understory stand biomass (leaf and stem) under eCO₂ conditions [45]. Moreover, increased

seedling biomass under eCO₂ conditions is associated with light availability [46]. However, the pot limitation effect can also limit the biomass incurred by eCO₂. In addition, *F. excelsior* and *Dactylis glomerata* seedlings showed marginal increases under eCO₂ conditions in a pot experiment, similar to our results [47].

N fertilization can cause an increase in net primary production in terrestrial ecosystems [48]; however, understory tree responses to N fertilization were not significant in some studies [49,50]. In addition, N fertilization significantly decreased the aboveground biomass of understory *Dicranopteris dichotoma* and *Lophatherum gracile* by 82.1% and 67.2%, respectively, compared with that under unfertilized treatments [51]. However, in our study, leaf and stem biomass were increased by N fertilization without an interaction effect between CO₂ and N (Figure 1). In summary, unlike overstory biomass, there was no increase in understory biomass under eCO₂ conditions owing to low light availability and the effect of N availability but without an interaction with eCO₂.

4.2. Down-Regulation of Photosynthesis and NSC under eCO₂ and N Fertilization

Tables 1 and 2 show reductions in leaf N and Rubisco contents under eCO₂ conditions, without an N fertilization effect, except in case of leaf N_{mass}. A previous meta-analysis showed that down-regulation of photosynthesis was associated with reduced leaf N_{mass} and Rubisco content under eCO₂ conditions [8,52]. Similar to the findings of other studies, leaf N and Rubisco contents also decreased under eCO₂ conditions in understory seedlings (Table 2) in our study; however, the differences in N_{mass} among CO₂ conditions decreased owing to retranslocation in September (Figure 2a). The dilution hypothesis suggests that down-regulation of photosynthesis is because of NSC accumulation resulting from a sink–source imbalance [11,53]. Yin [23] suggested that this sink–source imbalance can be mitigated by N fertilization under eCO₂ conditions; however, in our study, there were no interaction effects between N and CO₂ on J_{max}, Rubisco content, and NSC, and the differences in Rubisco content and NSC among CO₂ treatments were greater in N3 due to increased Rubisco content under aCO₂ conditions by N fertilization (Tables 1 and 2). Moreover, contrary to the dilution effect hypothesis, a reduction in NSC under eCO₂ 1.4 condition occurred in our study (Tables 1 and 2). Some studies have shown no differences in understory NSC under eCO₂ conditions, whereas NSC in a light-sufficient canopy increased under eCO₂ conditions. For example, the NSC of *Hedera helix* was consistently 60% higher under eCO₂ in the subcanopy; in contrast, leaves in the understory showed no differences in NSC between eCO₂ and aCO₂ conditions [54]. The accumulation of NSC increased noticeably with height in the canopy under eCO₂ conditions in 15 tropical species, suggesting that full solar illumination accelerates sink and source imbalances under eCO₂ conditions [45].

In addition, there was an interaction effect of CO₂ and time period, resulting in a greater decrease in NSC under eCO₂ conditions in September 2020, when leaf senescence started in the overstory and light availability increased in the understory (Table 1, Figure 2c). Therefore, decreased NSC under eCO₂ conditions in the understory was related to decreased leaf N concentration and low light availability, and down-regulation of photosynthesis was not caused by the accumulation of NSC in this study. Some studies have suggested that photosynthesis down-regulation cannot be explained entirely by sink size [55,56]. Bloom, et al. [57] and Wujeska-Klause, Crous, Ghannoum and Ellsworth [17] suggested that lower leaf N concentration under eCO₂ condition than under aCO₂ condition is driven by insufficient reductant from decreased photorespiration, resulting in reduced NO₃[−] assimilation compared with root absorption of NO₃[−].

Although photosynthesis was downregulated, A_{max} enhancement of understory saplings under eCO₂ conditions occurred for 2 years, regardless of N fertilization (Table 2). Similar to our results, Sefcik, et al. [58] reported that the long-term improvement of A_{max} under eCO₂ conditions was 97% for seedlings in deep shade and 47% for those in moderate shade compared with seedlings grown under CO₂ conditions. Similarly, several previ-

ous studies have reported that the impact of eCO₂ increases A_{\max} under light-limiting conditions [59–61].

4.3. PNUE and N Allocation under eCO₂ Conditions and N Fertilization

Increased PNUE is associated with the enhanced efficiency of Rubisco due to photorespiration suppression under eCO₂ conditions [8]. Similar to the findings of a previous study, PNUE increased under eCO₂ conditions regardless of N fertilization (Tables 1 and 2). In general, increased leaf N concentration was accompanied by decreased PNUE, but the increase in PNUE was sustained under eCO₂ conditions despite a high N supply, similar to our results [62,63]. Davey, Parsons, Atkinson, Wadge and Long [63] suggested that the eCO₂ effect may improve PNUE, independent of leaf N content. Increased PNUE under eCO₂ conditions was associated with the reallocation of leaf N from Rubisco to other photosynthetic apparatuses, such as light harvesting or electron transport enzymes [64]. However, there were no differences in the chlorophyll: Rubisco ratio among the CO₂ treatments (Table 1), and chlorophyll were reduced by the effect of eCO₂ (Table 2). In contrast to the findings of our study, other studies have noted an increase in chlorophyll under eCO₂ conditions [65]. In addition, a small decrease in Rubisco content via suppression of Rubisco small subunit (RBC) genes led to increased chlorophyll content under eCO₂ conditions [16]. In contrast, the chlorophyll content was significantly reduced under eCO₂ conditions in some seedling experiments [66,67].

4.4. Biochemical Changes in Sink Organs under eCO₂ and N Fertilization

Unlike the reduction of leaf N_{mass} under eCO₂ conditions, the stem N_{mass} under eCO₂ conditions increased compared with that under aCO₂ conditions, showing noticeable differences under N3 treatment in this study (Figure 3a). Root N_{mass} also showed a similar tendency, but the difference was not significant (Figure 3b). However, the average root N_{mass} under eCO₂ conditions decreased by 7.1% compared with that under aCO₂ conditions in a meta-analysis [68], and stem N_{mass} under eCO₂ conditions was also reduced in 11 species [69]. However, similar to the findings of our study, eCO₂ significantly increased the grain yield of rice crops in middle N and high N concentrations with a reduction of leaf N concentration under eCO₂ conditions, which was attributed to the increased N uptake under eCO₂ conditions being the highest at high N concentration [70].

Taub and Wang [19] suggested that the reduction of N_{mass} in whole plants can be attributed to the accumulation of NSC under eCO₂ conditions. In this study, the NSC of stems showed no differences among CO₂ treatments, except for N2, being lower under eCO₂1.4 than under aCO₂ (Figure 3c). For root NSC, there were no differences between the N and CO₂ treatments (Figure 3d). In the case of *Populus cathayana*, root starch significantly decreased under eCO₂ conditions compared with that under aCO₂ conditions under low N concentration, and stem starch increased under eCO₂ conditions in both N-fertilized and unfertilized conditions [71]. However, there were no changes in soluble sugar in aboveground woody parts and roots under eCO₂ conditions compared with those under aCO₂ conditions, whereas starch increased by 9.8% under elevated CO₂ conditions in 71 species in a meta-analysis. The NSC of roots and stems varied with species and growth conditions, and we concluded that the N_{mass} of roots and stems was not affected by the NSC of those parts in this study.

5. Conclusions

The reduction of leaf N and Rubisco contents decreased under eCO₂ conditions in the understory, but N fertilization could not mitigate this decrease. In addition, NSC decreased under eCO₂ conditions; this result contradicts that of previous overstory studies, wherein leaf NSC increased under eCO₂ conditions. The reduction of leaf N and Rubisco content was not caused by NSC accumulation, and decreased NSC was associated with insufficient light availability in the understory. Reduction of leaf N_{mass} could be related to PNUE improvement, resulting from reduced photorespiration driving less availability of

reductant in NO_3^- under eCO₂ conditions. Unlike leaf N, stem N increased under eCO₂ conditions, and there was no change in root N. The increase in stem N_{mass} might have been caused by increased N uptake under N fertilization treatment.

Author Contributions: Conceptualization, S.B. and H.S.K.; Methodology, S.-H.H. and C.O.; Investigation, K.K., J.H., S.K. (Seohyun Kim), S.K. (Sukyung Kim), C.P. and D.R.; Writing—Original Draft Preparation, S.B.; Writing—Review & Editing, S.B. and H.S.K.; Visualization, S.B.; Supervision, H.S.K.; Project Administration, H.S.K.; Funding Acquisition, H.S.K. All authors have read and agreed to the published version of the manuscript.

Funding: This research was funded by the National Research Foundation of Korea (grant numbers 2017R1A2B22012605 and 2014R1A1A2055127).

Acknowledgments: We would like to thank the Department of Forest Bioresources, the National Institute of Forest Science for their assistance.

Conflicts of Interest: The authors declare no conflict of interest.

References

1. Drake, B.G.; Gonzalez-Meler, M.A.; Long, S.P. More efficient plants: A consequence of rising atmospheric CO₂? *Annu. Rev. Plant Physiol. Plant Mol. Biol.* **1997**, *48*, 609–639. [[CrossRef](#)]
2. Reich, P.B.; Hobbie, S.E.; Lee, T.D.; Pastore, M.A. Unexpected reversal of C₃ versus C₄ grass response to elevated CO₂ during a 20-year field experiment. *Science* **2018**, *360*, 317–320. [[CrossRef](#)]
3. Ainsworth, E.A.; Long, S.P. What have we learned from 15 years of free-air CO₂ enrichment (FACE)? A meta-analytic review of the responses of photosynthesis, canopy properties and plant production to rising CO₂. *New Phytol.* **2005**, *165*, 351–372. [[CrossRef](#)]
4. Norby, R.J.; Warren, J.M.; Iversen, C.M.; Medlyn, B.E.; McMurtrie, R.E. CO₂ enhancement of forest productivity constrained by limited nitrogen availability. *Proc. Natl. Acad. Sci. USA* **2010**, *107*, 19368–19373. [[CrossRef](#)]
5. Jiang, M.; Medlyn, B.E.; Drake, J.E.; Duursma, R.A.; Anderson, I.C.; Barton, C.V.; Boer, M.M.; Carrillo, Y.; Castañeda-Gómez, L.; Collins, L. The fate of carbon in a mature forest under carbon dioxide enrichment. *Nature* **2020**, *580*, 227–231. [[CrossRef](#)]
6. Wang, S.; Zhang, Y.; Ju, W.; Chen, J.M.; Ciais, P.; Cescatti, A.; Sardans, J.; Janssens, I.A.; Wu, M.; Berry, J.A. Recent global decline of CO₂ fertilization effects on vegetation photosynthesis. *Science* **2020**, *370*, 1295–1300. [[CrossRef](#)]
7. Luo, Y.; Su, B.; Currie, W.S.; Dukes, J.S.; Finzi, A.C.; Hartwig, U.; Hungate, B.; McMurtrie, R.E.; Oren, R.; Parton, W.J.; et al. Progressive nitrogen limitation of ecosystem responses to rising atmospheric carbon dioxide. *Bioscience* **2004**, *54*, 731–739. [[CrossRef](#)]
8. Leakey, A.D.B.; Ainsworth, E.A.; Bernacchi, C.J.; Rogers, A.; Long, S.P.; Ort, D.R. Elevated CO₂ effects on plant carbon, nitrogen, and water relations: Six important lessons from FACE. *J. Exp. Bot.* **2009**, *60*, 2859–2876. [[CrossRef](#)]
9. Evans, J.R. Photosynthesis and nitrogen relationships in leaves of C₃ plants. *Oecologia* **1989**, *78*, 9–19. [[CrossRef](#)]
10. Moore, B.; Cheng, S.H.; Sims, D.; Seemann, J. The biochemical and molecular basis for photosynthetic acclimation to elevated atmospheric CO₂. *Plant Cell Environ.* **1999**, *22*, 567–582. [[CrossRef](#)]
11. Ainsworth, E.A.; Rogers, A.; Nelson, R.; Long, S.P. Testing the “source–sink” hypothesis of down-regulation of photosynthesis in elevated [CO₂] in the field with single gene substitutions in *Glycine max*. *Agric. For. Meteorol.* **2004**, *122*, 85–94. [[CrossRef](#)]
12. Hovenden, M.J. Photosynthesis of coppicing poplar clones in a free-air CO₂ enrichment (FACE) experiment in a short-rotation forest. *Funct. Plant Biol.* **2003**, *30*, 391–400. [[CrossRef](#)]
13. Kelly, A.A.; van Erp, H.; Quettier, A.-L.; Shaw, E.; Menard, G.; Kurup, S.; Eastmond, P.J. The sugar-dependent1 lipase limits triacylglycerol accumulation in vegetative tissues of *Arabidopsis*. *Plant Physiol.* **2013**, *162*, 1282–1289. [[CrossRef](#)]
14. Sugiura, D.; Watanabe, C.K.; Betsuyaku, E.; Terashima, I. Sink–source balance and down-regulation of photosynthesis in *Raphanus sativus*: Effects of grafting, N and CO₂. *Plant Cell Physiol.* **2017**, *58*, 2043–2056. [[CrossRef](#)] [[PubMed](#)]
15. Ruiz-Vera, U.M.; De Souza, A.P.; Long, S.P.; Ort, D.R. The role of sink strength and nitrogen availability in the down-regulation of photosynthetic capacity in field-grown *Nicotiana tabacum* L. at elevated CO₂ concentration. *Front. Plant Sci.* **2017**, *8*, 998. [[CrossRef](#)]
16. Kanno, K.; Suzuki, Y.; Makino, A. A small decrease in Rubisco content by individual suppression of RBCS genes leads to improvement of photosynthesis and greater biomass production in rice under conditions of elevated CO₂. *Plant Cell Physiol.* **2017**, *58*, 635–642. [[CrossRef](#)]
17. Wujeska-Klause, A.; Crous, K.Y.; Ghannoum, O.; Ellsworth, D.S. Lower photorespiration in elevated CO₂ reduces leaf N concentrations in mature Eucalyptus trees in the field. *Glob. Chang. Biol.* **2019**, *25*, 1282–1295. [[CrossRef](#)]
18. Gifford, R.M.; Barrett, D.J.; Lutze, J.L. The effects of elevated [CO₂] on the C:N and C:P mass ratios of plant tissues. *Plant Soil* **2000**, *224*, 1–14. [[CrossRef](#)]
19. Taub, D.R.; Wang, X. Why are nitrogen concentrations in plant tissues lower under elevated CO₂? A critical examination of the hypotheses. *J. Integr. Plant Biol.* **2008**, *50*, 1365–1374. [[CrossRef](#)] [[PubMed](#)]

20. Taub, D.R.; Miller, B.; Allen, H. Effects of elevated CO₂ on the protein concentration of food crops: A meta-analysis. *Glob. Chang. Biol.* **2008**, *14*, 565–575. [[CrossRef](#)]
21. Wang, L.; Feng, Z.; Schjoerring, J.K. Effects of elevated atmospheric CO₂ on physiology and yield of wheat (*Triticum aestivum* L.): A meta-analytic test of current hypotheses. *Agric. Ecosyst. Environ.* **2013**, *178*, 57–63. [[CrossRef](#)]
22. Li, W.; Hartmann, H.; Adams, H.D.; Zhang, H.; Jin, C.; Zhao, C.; Guan, D.; Wang, A.; Yuan, F.; Wu, J. The sweet side of global change—dynamic responses of non-structural carbohydrates to drought, elevated CO₂ and nitrogen fertilization in tree species. *Tree Physiol.* **2018**, *38*, 1706–1723. [[CrossRef](#)]
23. Yin, X. Responses of leaf nitrogen concentration and specific leaf area to atmospheric CO₂ enrichment: A retrospective synthesis across 62 species. *Glob. Chang. Biol.* **2002**, *8*, 631–642. [[CrossRef](#)]
24. Bazzaz, F.; Miao, S. Successional Status, Seed Size, and Responses of Tree Seedlings to CO₂, Light, and Nutrients. *Ecology* **1993**, *74*, 104–112. [[CrossRef](#)]
25. Sholtis, J.D.; Gunderson, C.A.; Norby, R.J.; Tissue, D.T. Persistent stimulation of photosynthesis by elevated CO₂ in a sweetgum (*Liquidambar styraciflua*) forest stand. *New Phytol.* **2004**, *162*, 343–354. [[CrossRef](#)]
26. Ellsworth, D.S.; Reich, P.B.; Naumburg, E.S.; Koch, G.W.; Kubiske, M.E.; Smith, S.D. Photosynthesis, carboxylation and leaf nitrogen responses of 16 species to elevated pCO₂ across four free-air CO₂ enrichment experiments in forest, grassland and desert. *Glob. Chang. Biol.* **2004**, *10*, 2121–2138. [[CrossRef](#)]
27. Kerstiens, G. Meta-analysis of the interaction between shade-tolerance, light environment and growth response of woody species to elevated CO₂. *Acta Oecol.* **2001**, *22*, 61–69. [[CrossRef](#)]
28. Dirnböck, T.; Kraus, D.; Grote, R.; Klatt, S.; Kobler, J.; Schindlbacher, A.; Seidl, R.; Thom, D.; Kiese, R. Substantial understory contribution to the C sink of a European temperate mountain forest landscape. *Landsc. Ecol.* **2020**, *35*, 483–499. [[CrossRef](#)]
29. Wu, J.; Liu, Z.; Chen, D.; Huang, G.; Zhou, L.; Fu, S. Understory plants can make substantial contributions to soil respiration: Evidence from two subtropical plantations. *Soil Biol. Biochem.* **2011**, *43*, 2355–2357. [[CrossRef](#)]
30. Stocker, T.F.; Qin, D.; Plattner, G.-K.; Tignor, M.; Allen, S.K.; Boschung, J.; Nauels, A.; Xia, Y.; Bex, V.; Midgley, P.M. Climate Change 2013: The Physical Science Basis. In *Contribution of Working Group I to the Fifth Assessment Report of the Intergovernmental Panel on Climate Change*; Cambridge University Press: Cambridge, UK, 2013; Volume 1535.
31. Lee, J.-C.; Kim, D.-H.; Kim, G.-N.; Kim, P.-G.; Han, S.-H. Long-term climate change research facility for trees: CO₂-enriched open top chamber system. *Korean J. Agric. For. Meteorol.* **2012**, *14*, 19–27. [[CrossRef](#)]
32. Eriksson, H.; Eklundh, L.; Hall, K.; Lindroth, A. Estimating LAI in deciduous forest stands. *Agric. For. Meteorol.* **2005**, *129*, 27–37. [[CrossRef](#)]
33. Billings, S.A.; Ziegler, S.E. Altered patterns of soil carbon substrate usage and heterotrophic respiration in a pine forest with elevated CO₂ and N fertilization. *Glob. Chang. Biol.* **2008**, *14*, 1025–1036. [[CrossRef](#)]
34. Kitao, M.; Löw, M.; Heerdt, C.; Grams, T.E.; Häberle, K.-H.; Matyssek, R. Effects of chronic elevated ozone exposure on gas exchange responses of adult beech trees (*Fagus sylvatica*) as related to the within-canopy light gradient. *Environ. Pollut.* **2009**, *157*, 537–544. [[CrossRef](#)] [[PubMed](#)]
35. Larcher, W. *Physiological Plant Ecology: Ecophysiology and Stress Physiology of Functional Groups*; Springer Science & Business Media, Institute of Botany University of Innsbruck Sternwartestrasse: Innsbruck, Austria, 2003.
36. Sharkey, T.D. What gas exchange data can tell us about photosynthesis. *Plant Cell Environ.* **2016**, *39*, 1161–1163. [[CrossRef](#)] [[PubMed](#)]
37. Ashwell, G. New colorimetric methods of sugar analysis. In *Methods in Enzymology*; Elsevier, Michigan State University: East Lansing, MI, USA, 1966; Volume 8, pp. 85–95.
38. Hikosaka, K.; Shigeno, A. The role of Rubisco and cell walls in the interspecific variation in photosynthetic capacity. *Oecologia* **2009**, *160*, 443–451. [[CrossRef](#)]
39. Shinano, T.; Lei, T.; Kawamukai, T.; Inoue, M.; Koike, T.; Tadano, T. Dimethylsulfoxide method for the extraction of chlorophylls a and b from the leaves of wheat, field bean, dwarf bamboo, and oak. *Photosynthetica* **1996**, *32*, 409–415.
40. Wellburn, A.R. The spectral determination of chlorophylls a and b, as well as total carotenoids, using various solvents with spectrophotometers of different resolution. *J. Plant Physiol.* **1994**, *144*, 307–313. [[CrossRef](#)]
41. van der Kooi, C.J.; Reich, M.; Löw, M.; De Kok, L.J.; Tausz, M. Growth and yield stimulation under elevated CO₂ and drought: A meta-analysis on crops. *Environ. Exp. Bot.* **2016**, *122*, 150–157. [[CrossRef](#)]
42. McCarthy, H.R.; Oren, R.; Johnsen, K.H.; Gallet-Budynek, A.; Pritchard, S.G.; Cook, C.W.; LaDeau, S.L.; Jackson, R.B.; Finzi, A.C. Re-assessment of plant carbon dynamics at the Duke free-air CO₂ enrichment site: Interactions of atmospheric [CO₂] with nitrogen and water availability over stand development. *New Phytol.* **2010**, *185*, 514–528. [[CrossRef](#)]
43. Ryan, M.G. Three decades of research at Flakaliden advancing whole-tree physiology, forest ecosystem and global change research. *Tree Physiol.* **2013**, *33*, 1123–1131. [[CrossRef](#)]
44. Souza, L.; Belote, R.T.; Kardol, P.; Weltzin, J.F.; Norby, R.J. CO₂ enrichment accelerates successional development of an understory plant community. *J. Plant Ecol.* **2010**, *3*, 33–39. [[CrossRef](#)]
45. Körner, C.; Arnone, J.A. Responses to elevated carbon dioxide in artificial tropical ecosystems. *Science* **1992**, *257*, 1672–1675. [[CrossRef](#)] [[PubMed](#)]
46. Hättenschwiler, S.e.; Körner, C.r. Tree seedling responses to in situ CO₂-enrichment differ among species and depend on understorey light availability. *Glob. Chang. Biol.* **2000**, *6*, 213–226. [[CrossRef](#)]

47. Bloor, J.; Barthes, L.; Leadley, P.W. Effects of elevated CO₂ and N on tree–grass interactions: An experimental test using *Fraxinus excelsior* and *Dactylis glomerata*. *Funct. Ecol.* **2008**, *22*, 537–546. [[CrossRef](#)]
48. LeBauer, D.S.; Treseder, K.K. Nitrogen limitation of net primary productivity in terrestrial ecosystems is globally distributed. *Ecology* **2008**, *89*, 371–379. [[CrossRef](#)]
49. Tian, D.; Li, P.; Fang, W.; Xu, J.; Luo, Y.; Yan, Z.; Zhu, B.; Wang, J.; Xu, X.; Fang, J. Growth responses of trees and understory plants to nitrogen fertilization in a subtropical forest in China. *Biogeosciences* **2017**, *14*, 3461–3469. [[CrossRef](#)]
50. Son, Y.; Lee, M.-H.; Noh, N.J.; Kang, B.H.; Kim, K.O.; Yi, M.J.; Byun, J.K.; Yi, K. Fertilization effects on understory vegetation biomass and structure in four different plantations. *J. Korean Soc. For. Sci.* **2007**, *96*, 520–527.
51. Wang, F.; Chen, F.; Wang, G.G.; Mao, R.; Fang, X.; Wang, H.; Bu, W. Effects of experimental nitrogen addition on nutrients and nonstructural carbohydrates of dominant understory plants in a Chinese fir plantation. *Forests* **2019**, *10*, 155. [[CrossRef](#)]
52. Rogers, A.; Ellsworth, D.S. Photosynthetic acclimation of *Pinus taeda* (loblolly pine) to long-term growth in elevated pCO₂ (FACE). *Plant Cell Environ.* **2002**, *25*, 851–858. [[CrossRef](#)]
53. Stitt, M.; Krapp, A. The interaction between elevated carbon dioxide and nitrogen nutrition: The physiological and molecular background. *Plant Cell Environ.* **1999**, *22*, 583–621. [[CrossRef](#)]
54. Zottz, G.; Cueni, N.; Körner, C. In situ growth stimulation of a temperate zone liana (*Hedera helix*) in elevated CO₂. *Funct. Ecol.* **2006**, *20*, 763–769. [[CrossRef](#)]
55. Ziska, L.H.; Bunce, J.A. Sensitivity of field-grown soybean to future atmospheric CO₂: Selection for improved productivity in the 21st century. *Funct. Plant Biol.* **2000**, *27*, 979–984. [[CrossRef](#)]
56. Ziska, L.H.; Bunce, J.A.; Caulfield, F.A. Rising atmospheric carbon dioxide and seed yield of soybean genotypes. *Crop Sci.* **2001**, *41*, 385–391. [[CrossRef](#)]
57. Bloom, A.J.; Burger, M.; Asensio, J.S.R.; Cousins, A.B. Carbon dioxide enrichment inhibits nitrate assimilation in wheat and *Arabidopsis*. *Science* **2010**, *328*, 899–903. [[CrossRef](#)]
58. Sefcik, L.T.; Zak, D.R.; Ellsworth, D.S. Photosynthetic responses to understory shade and elevated carbon dioxide concentration in four northern hardwood tree species. *Tree Physiol.* **2006**, *26*, 1589–1599. [[CrossRef](#)]
59. Hättenschwiler, S. Tree seedling growth in natural deep shade: Functional traits related to interspecific variation in response to elevated CO₂. *Oecologia* **2001**, *129*, 31–42. [[CrossRef](#)] [[PubMed](#)]
60. Leakey, A.; Press, M.C.; Scholes, J.; Watling, J. Relative enhancement of photosynthesis and growth at elevated CO₂ is greater under sunflecks than uniform irradiance in a tropical rain forest tree seedling. *Plant Cell Environ.* **2002**, *25*, 1701–1714. [[CrossRef](#)]
61. Granados, J.; Körner, C. In deep shade, elevated CO₂ increases the vigor of tropical climbing plants. *Glob. Chang. Biol.* **2002**, *8*, 1109–1117. [[CrossRef](#)]
62. Novriyanti, E.; Watanabe, M.; Kitao, M.; Utsugi, H.; Uemura, A.; Koike, T. High nitrogen and elevated [CO₂] effects on the growth, defense and photosynthetic performance of two eucalypt species. *Environ. Pollut.* **2012**, *170*, 124–130. [[CrossRef](#)]
63. Davey, P.; Parsons, A.; Atkinson, L.; Wadge, K.; Long, S.P. Does photosynthetic acclimation to elevated CO₂ increase photosynthetic nitrogen-use efficiency? A study of three native UK grassland species in open-top chambers. *Funct. Ecol.* **1999**, *13*, 21–28. [[CrossRef](#)]
64. Evans, J.R.; Seemann, J.R. The allocation of protein nitrogen in the photosynthetic apparatus: Costs, consequences, and control. *Photosynthesis* **1989**, *8*, 183–205.
65. Choi, D.; Watanabe, Y.; Guy, R.D.; Sugai, T.; Toda, H.; Koike, T. Photosynthetic characteristics and nitrogen allocation in the black locust (*Robinia pseudoacacia* L.) grown in a FACE system. *Acta Physiol. Plant.* **2017**, *39*. [[CrossRef](#)]
66. Sallas, L.; Luomala, E.-M.; Utriainen, J.; Kainulainen, P.; Holopainen, J.K. Contrasting effects of elevated carbon dioxide concentration and temperature on Rubisco activity, chlorophyll fluorescence, needle ultrastructure and secondary metabolites in conifer seedlings. *Tree Physiol.* **2003**, *23*, 97–108. [[CrossRef](#)] [[PubMed](#)]
67. Zhao, X.; Mao, Z.; Xu, J. Gas exchange, chlorophyll and growth responses of *Betula Platypylla* seedlings to elevated CO₂ and nitrogen. *Int. J. Biol.* **2010**, *2*, 143. [[CrossRef](#)]
68. Nie, M.; Lu, M.; Bell, J.; Raut, S.; Pendall, E. Altered root traits due to elevated CO₂: A meta-analysis. *Glob. Ecol. Biogeogr.* **2013**, *22*, 1095–1105. [[CrossRef](#)]
69. Cotrufo, M.F.; Ineson, P.; Scott, A. Elevated CO₂ reduces the nitrogen concentration of plant tissues. *Glob. Change Biol.* **1998**, *4*, 43–54. [[CrossRef](#)]
70. Kim, H.Y.; Lieffering, M.; Kobayashi, K.; Okada, M.; Miura, S. Seasonal changes in the effects of elevated CO₂ on rice at three levels of nitrogen supply: A free air CO₂ enrichment (FACE) experiment. *Glob. Change Biol.* **2003**, *9*, 826–837. [[CrossRef](#)]
71. Zhao, H.; Xu, X.; Zhang, Y.; Korpelainen, H.; Li, C. Nitrogen deposition limits photosynthetic response to elevated CO₂ differentially in a dioecious species. *Oecologia* **2011**, *165*, 41–54. [[CrossRef](#)] [[PubMed](#)]